This is an author produced version of a paper published in **Physics of Plasmas**.

White Rose Research Online URL for this paper:
http://eprints.whiterose.ac.uk/42647

Torsional magnetic reconnection at 3D null points: A phenominological study

Peter Wyper and Rekha Jain

School of Mathematics and Statistics, University of Sheffield, Sheffield, S3 7RH, UK

Magnetic reconnection around three dimensional (3D) magnetic null points is the natural progression from X-point reconnection in two dimensions. In 3D the separator field lines of the X-point are replaced with the spine line and fan plane (the field lines which asymptotically approach or recede from the null). In this work analytical models are developed for the newly classified *Torsional spine* and *Torsional fan* reconnection regimes by solving the steady state, kinematic, resistive magneto-hydrodynamic (MHD) equations. Reconnection is localised to around the null through the use of a localised field perturbation leading to a localised current whilst a constant resistivity is assumed.

For the torsional spine case current is found to localise around the spine leading to a spiraling slippage of the field around the spine and out along the fan. For the torsional fan case current is found to be localised to the fan plane leading again to a spiraling slippage of the field. In each case no flux is transported across either the spine or the fan.

An intermediate twist is then introduced and a link is established between the two regimes. We find that for a general twist plasma flows associated with both torsional spine and fan appear in distinct regions. As such we suggest that the 'pure' flows of each are extreme cases.

PACS numbers:

I. INTRODUCTION

Magnetic reconnection is a fundamental physical process of an astrophysical plasma. It is the restructuring of the magnetic field through the breaking and changing of the connectivity of the magnetic field lines. The majority of astrophysical plasmas including the solar corona, however have a low plasma resistivity so reconnection may only occur in regions where very intense currents develop. Therefore the key questions regarding reconnection in astrophysical plasmas are where do these intense currents develop and what effects do they have on the plasma flows and energy release?

This however is not an easy problem since the astrophysical plasmas have a very complex 3D magnetic structure. Recent efforts to understand magnetic reconnection in solar corona have led to some progress. Two main scenarios have emerged during the investigation of the current sheet formation process: reconnection at and around 3D magnetic null points and their associated separator field lines - the field line that connects two nulls (for example, [2, 3, 5–9, 17, 20]). We focus here on reconnection around an isolated 3D null. The field topology in the vicinity of such a null is defined by two structures. The *fan* (or Σ-) plane: a continuum of field lines that asymptotically recede from (or approach) the null and the *spine* (or γ-) line: two field lines that asymptotically approach (or recede from) the null. These structures may be found by examining the linearised field topology around the null defined by the equation

$$\mathbf{B} = \mathcal{M} \cdot \mathbf{r} \tag{1}$$

where the matrix $\mathcal{M}$ is given by the Jacobian of $\mathbf{B}$ and $\mathbf{r}$ the position vector $(x, y, z)^T$. The eigenvectors of $\mathcal{M}$ (whose corresponding eigenvalues sum to zero since $\nabla \cdot \mathbf{B} = 0$) define the spine and fan such that the two eigenvalues whose real parts have like sign lie in the fan plane with the third directed along the spine line. The fan surface is a separatrix surface between two topologically unique regions. The spine can not separate different regions being only a line but is still an important feature as changes in the symmetry within the regions separated by the fan manifest in a change in the field at or around the spine.

The existence of 3D nulls is predicted in abundance in the solar corona (e.g [10, 11, 22]). Proposed applications for null reconnection include sites for coronal heating ([21]) and involvement in jets ([14, 23]), solar flares ([12, 13]) and coronal mass ejections ([24], [1]). The evidence for 3D null point reconnection is also suggested in the Earth's magnetotail on the basis of observations from the cluster satellites [25].

Although it is now accepted that reconnection at 3D null points is of great importance in realistic 3D field geometries, a full understanding of the different kinds of reconnection that occur at these null points, is still to be achieved. Early work using ideal steady state kinematic models [5, 20] suggested reconnection types that transported flux across the fan or spine. Later work by [15, 16] extended this to include a local diffusion region and constant current $\mathbf{J}$. Two different current cases were considered. When $\mathbf{J}$ was parallel to the fan plane flux was found to cross both the spine and fan in a similar way as was suggested by [20]. When $\mathbf{J}$ was parallel to the spine however a rotational slippage

of the field was found where no flux was transported across either the spine or fan but rotated around the spine symmetrically. Numerical experiments by [18] and [4] also found this rotational slippage but with currents diffused in one direction when the magnetic field is rotationally perturbed. Pontin and Galsgaard [18] also noted that perturbing the fan or spine produced local currents focusing on the null with plasma flow across the fan or spine respectively. The culmination of all these results led Pontin and Priest [19] to reclassify reconnection around 3D nulls into three types: *Torsional Fan* and *Torsional Spine* which involve spatially diffused currents in one direction leading to rotational slippage and *Spine-Fan* which covers all cases of flux transport across the spine or fan in the more traditional manner.

As noted, so far, all the steady state, kinematic models have been studied by localising η. However, from simulation studies (for example, [4] and [18]), localised currents have been seen with slippage of flux velocities around the spine and fan, and for applications to Astrophysical plasma, it may also be interesting to explore the effect of localised current. This work aims to present steady kinematic models for Torsional Spine and Torsional Fan through the use of a localised current.

II. GENERAL METHOD

We seek to find solutions to the kinematic, steady state, resistive MHD equations in the vicinity of a 3D magnetic null point. Thus, we solve

$$
\begin{align}
\mathbf{E} + \mathbf{v} \times \mathbf{B} &= \eta \mathbf{J}, \tag{2}\\
\nabla \times \mathbf{E} &= 0, \tag{3}\\
\nabla \times \mathbf{B} &= \mu_0 \mathbf{J}, \tag{4}\\
\nabla \cdot \mathbf{B} &= 0. \tag{5}
\end{align}
$$

From equation (3) we can express the electric field as $\mathbf{E} = -\nabla\Phi$ where Φ is a scalar potential. The component of equation (2) parallel to $\mathbf{B}$ can be combined with this and integrated along the magnetic field lines to give

$$
\Phi = -\int \eta \mathbf{J} \cdot \mathbf{B} \, \mathbf{ds} + \Phi_0. \tag{6}
$$

This integral is solved by using the field lines equations in (r, ϕ, z) expressed in terms of the parameter s and some initial position (r_0, ϕ_0, z_0). The field line equations are obtained by solving

$$
\frac{dr}{B_r} = \frac{r d\phi}{B_\phi} = \frac{dz}{B_z} = ds. \tag{7}
$$

These equations are invertible so Φ can be represented as a function of s and initial position to carry out the integral in equation (6) and then transferred back into a function of r, ϕ and z to find the electric field from

$$
\mathbf{E} = -\nabla\Phi. \tag{8}
$$

Thus for a given magnetic configuration we can find the electric field due to non-ideal effects (i.e. those due to $\mathbf{J} \neq \mathbf{0}$). Using this we can also find the resulting flow velocity perpendicular to the magnetic field by taking the vector product of equation (2) with $\mathbf{B}$ to give

$$
\mathbf{v}_\perp = \frac{(\mathbf{E} - \eta \mathbf{J}) \times \mathbf{B}}{B^2}. \tag{9}
$$

In the next section, we consider a general perturbation in the ϕ-component of a simple linear magnetic field and investigate the properties of torsional reconnections using this general method.

III. TORSIONAL RECONNECTION

Consider

$$
\mathbf{B} = B_0 \left(r, \, j r^\alpha z^\gamma (z r^2)^\beta e^{-\frac{1}{l^2}(a^2 r^2 + b^2 z^2 + c^2 (z r^2)^2)}, \, -2z \right) \tag{10}
$$

where α, β and γ are all either zero or positive integers and a, b, c, l and j are constants. This type of perturbation leads to a twist of the field lines around the spine and depending on the choice of parameters, rotational slippage of the field lines. In the following subsections, we investigate in detail, the two main types of torsional reconnections.

A. Torsional Spine

Consider the case $\gamma = 0$ and $a = 1$; $b = 0$ in the above equation (10). Thus the field is of the form:

$$\mathbf{B} = B_0 \left(r, jr^\alpha (zr^2)^\beta e^{-\frac{1}{l^2}(r^2 + c^2(zr^2)^2)}, -2z \right). \tag{11}$$

The field line equations for r and z can be found to be

$$r = r_0 e^{B_0 s}, \quad z = z_0 e^{-2B_0 s}. \tag{12}$$

Using these we can express the ϕ field line as

$$\phi = jB_0(z_0 r_0^2)^\beta e^{-\frac{c^2}{l^2}(z_0 r_0^2)^2} F(\alpha - 1) + C \tag{13}$$

where C is a constant of integration and $F(A)$ is defined as

$$F(A) = r_0^A \int e^{AB_0 s} e^{-\frac{r_0^2}{l^2} e^{2B_0 s}} ds. \tag{14}$$

Using integration by parts, it is easy to show a recurrence relation for F defined by

$$F(A + 2) = \frac{l^2}{2} \left(AF(A) - \frac{r^A}{B_0} e^{-\frac{r^2}{l^2}} \right) \tag{15}$$

and since

$$F(1) = \frac{l\sqrt{\pi}}{2B_0} \mathbf{erf} \left(\frac{r}{l} \right)$$

$$F(2) = -\frac{l^2 e^{-\frac{r^2}{l^2}}}{2B_0}$$

and the fact that $\alpha \geq 0$, we can find non-singular fields. Here $\mathbf{erf}\,(\mathbf{x})$ is an error function. Using equation (4) we find

$$\mathbf{J} = \frac{jB_0}{\mu_0} \left(z^{-1} \left(-\beta + \frac{2c^2}{l^2}(zr^2)^2 \right), 0, r^{-1} \left((2\beta + \alpha + 1) - \frac{2}{l^2}(r^2 + 2c^2(zr^2)^2) \right) \right) r^\alpha (zr^2)^\beta e^{-\frac{1}{l^2}(r^2 + c^2(zr^2)^2)} \tag{16}$$

and using equation (6) we find the electric potential

$$\Phi = \frac{j\eta_0 B_0}{\mu_0} \left[\left(\beta - \frac{2c^2}{l^2}(zr^2)^2 \right) F(\alpha + 3)(zr^2)^{\beta - 1} - \frac{4}{l^2} F(\alpha - 1)(zr^2)^{\beta + 1} \right.$$

$$\left. + \ 2 \left((\alpha + 2\beta + 1) - \frac{4c^2}{l^2}(zr^2)^2 \right) F(\alpha - 3)(zr^2)^{\beta + 1} \right] e^{-\frac{c^2}{l^2}(zr^2)} \tag{17}$$

where $\alpha \neq 1$ or 3.

It is clear that depending on the choice of parameters the field will be perturbed differently. In the following subsections we investigate in more detail the reconnection process that occurs for these different types of perturbation.

Throughout the paper unless otherwise stated we shall consider $l = \eta_0 = \mu_0 = B_0 = 1$ with the plots being produced using Maple 13 with a relative scaling of $(\text{strength/maximum})^{1/d}$ (where $d = 3$ unless otherwise stated) for clarity.

1. Same direction twist

For the field lines to be symmetric above and below the fan plane we must choose β to be *even* in conjunction with $\alpha > 0$, when $\alpha = 0$ all values of β give rise to sinks and sources, such flows are unphysical.

The z independent case: $\beta = 0$, $c = 0$.

Note from equation (17) that for $\beta = 0$, the z-component of the electric field $\left(E_z = -\frac{\partial \Phi}{\partial z} \right)$ is zero when
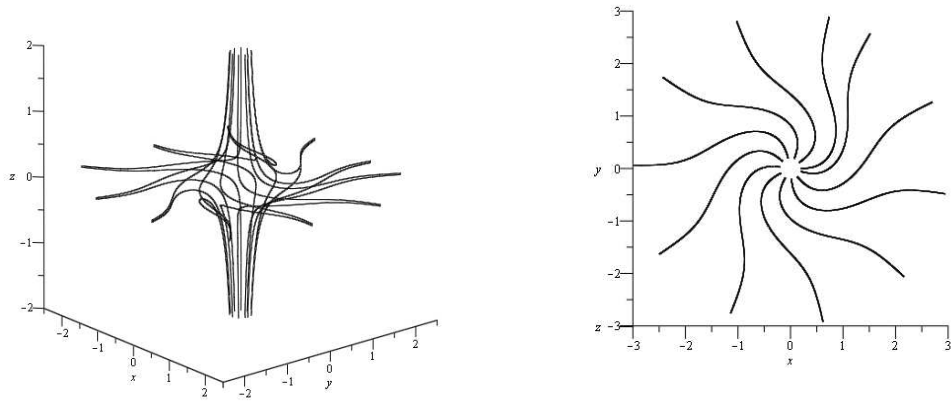
FIG. 1: Top and side view of field lines plotted for $\alpha = 4$ and $\beta = 0$ with $j = 3$. The field lines close to the spine are approaching the null and receding away from the null in the fan plane.
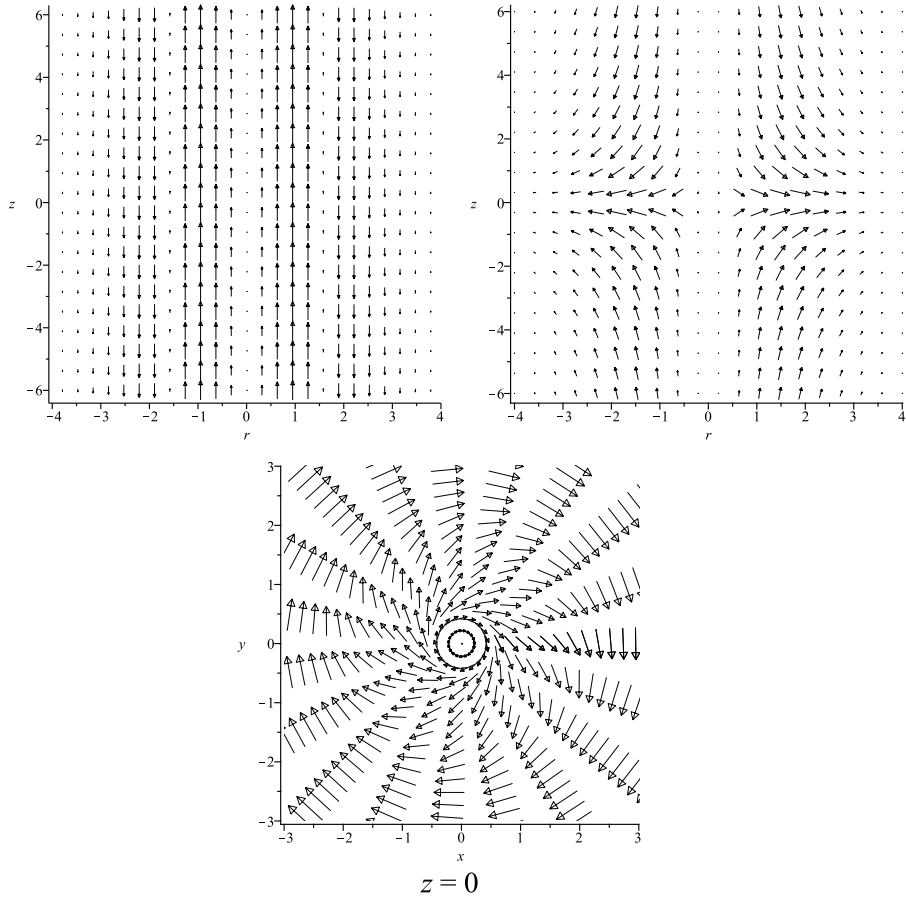

$$z = 0$$

FIG. 2: The left panel shows a slice of the radially symmetric current flow. The middle and right panels are the scaled plots of the plasma flow. These are plotted for $\alpha = 4$ and $\beta = 0$ with $j = 3$.
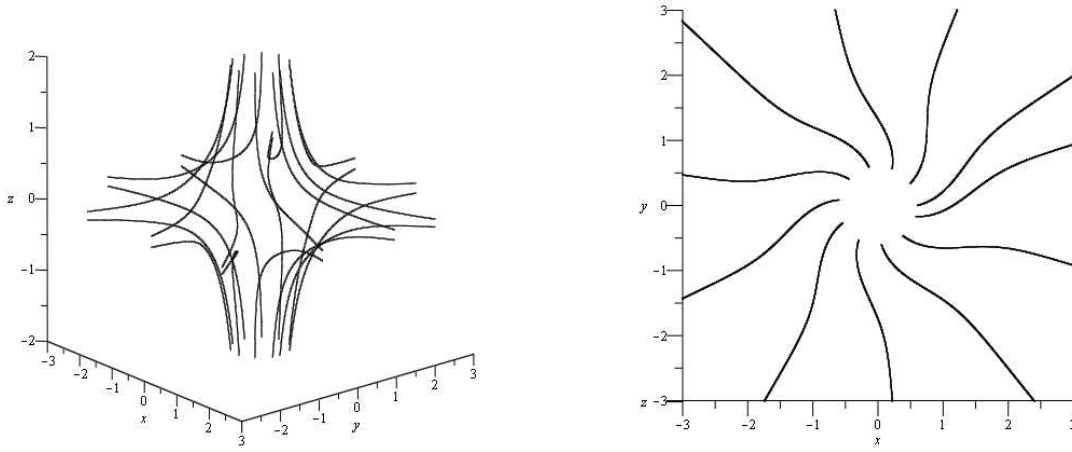
FIG. 3: Top and side view of field lines plotted for $\alpha = 4$, $\beta = 2$ and $c = 0.2$ with $j = 3$. The field lines close to the spine line are approaching the null and receding away from the null in the fan plane.

$\frac{F(\alpha-3)}{F(\alpha-1)} = \frac{2}{(\alpha+1)l^2}$ for $r \neq 0$. The total plasma flows, therefore have sinks and sources in the rz-plane for all odd α values. Such flows are unphysical. From equation (16) it is clear that for $\beta = 0$ a singular current results from $\alpha = 0$. Also, $\alpha = 2$ gives a non-zero $v_{\perp\phi}$ when $r = 0$ which is not a realistic physical solution. Thus, for $\beta = 0$, only even values of $\alpha \geq 4$ are permissible.

Even α

Using $\alpha = 4$ we get a field of the form

$$\mathbf{B} = B_0 \left(r, jr^4 e^{-\frac{r^2}{l^2}}, -2z \right). \tag{18}$$

Figure 1 shows the resulting twisted field-lines associated with this choice of parameters. We see a radially symmetric twist in the field that is localised to a toroidal region around the spine but which is unbounded in height. The value of l varies the strength of the damping from the exponential term which will stretch the toroidal region inward or outward. Outside the region we see the field lines straighten out as the field becomes more potential in nature. The current flows are found to be localised to the region of twist and exist in annular bands around the spine. Figure 2, left panel shows them as opposite bands in the rz-plane. Such bands were also observed at intermediate time steps in the numerical simulations by [18]. Recall that in our model, there is no current at the null itself so the field and the flows are more representative of the later stages of evolution after an initial disturbance.

Lastly, in the middle and right panels of Figure 2 we show the plasma velocity resulting from the twisting of the field lines. It appears that the plasma spirals down around the spine and then spirals out along the fan plane. As expected, the strongest flows occur within the region of greatest twist. For higher even values of α, the twist in the field is reduced (increased) where $r < l$ ($r > l$), with similar plasma and current flows. This kind of reconnection was also seen in the numerical simulation studies carried out by [18]. They also find rotational plasma flows but their flows were affected by reflections of the pulse from the simulation box boundary creating counter rotating flows which we don't see here.

The z dependent case: $\beta \neq 0$ and $c \neq 0$.

For this case, the twist in the field lines is localised to around the spine and near the fan whilst being zero in the fan plane. In order to have a symmetric twist above and below the fan plane, even values of β must be chosen. As we wish to study a smooth transition from z independence to z dependence we choose to keep $\alpha \geq 4$ for $\beta \neq 0$
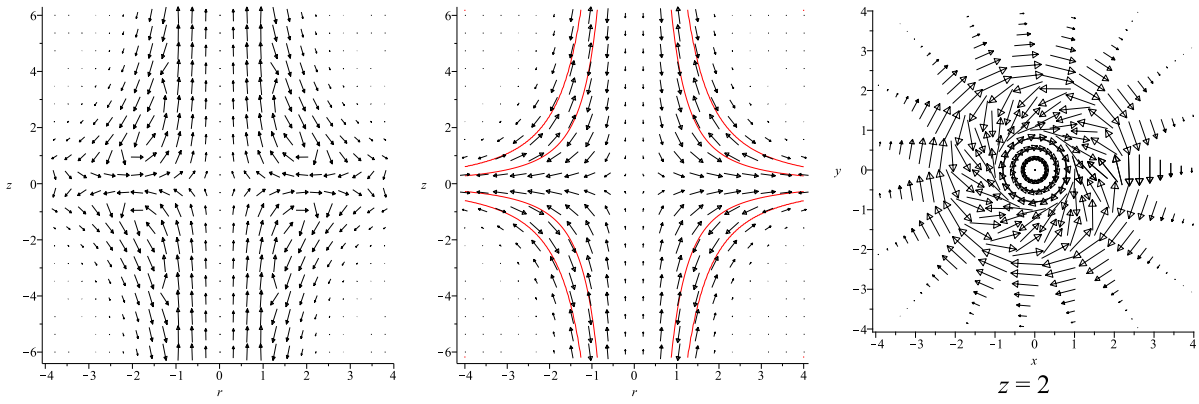
FIG. 4: Scaled plots of the radially symmetric current flow (left panel) and plasma flows (middle and right panels) for $\alpha = 4$, $\beta = 2$ and $c = 0.2$ with $l = 1$ and $j = 3$. Here, the maple scaling is applied with $d = 13$.

also. So we start with a field of the form

$$\mathbf{B} = B_0 \left(r, jz^2 r^8 e^{-\frac{r^2}{l^2} - \frac{c^2}{l^2}(zr^2)^2}, -2z \right), \tag{19}$$

where we have chosen $\alpha = 4$ and $\beta = 2$ whilst including a non-zero c value to maintain localisation.

Figure 3 shows the twist in the field that is again focused to a toroidal region around the spine with potential field surrounding it. However now the region has been pinched at the top and bottom by $c \neq 0$ and split to either side of the fan plane by the z power dependence ($\beta \neq 0$). Thus, on the fan itself the field lines are of potential form with the twist in the field existing in two tori either side of it. The shape of these regions is clearly outlined by the shape of the current flow shown in the left panel of Figure 4. We see that it is oppositely directed above and below the fan plane and flows in a circuit within these squashed tori.

Figure 4, right and middle panels, shows the plasma flow which we see is also localised to these shaped regions with an extra counter rotating flow (marked out in red) that takes plasma in along the fan and out along the spine. This region is introduced by the extra damping due to $c \neq 0$ in the exponential term in equation (19). Another interesting aspect of this flow is that there is no outflow of plasma in the fan plane, even though because of the co-rotating nature of the plasma either side of this plane the plasma rotates around within it. This is a consequence of the z power dependence ($\beta \neq 0$).

We also find that because the perturbation is a multiple of r^2 all other higher *even* values of α give similar results. Note that for odd values of α, the z-component of the electric field has sinks and sources for $r \neq 0$, which is unphysical.

2. Opposite direction twist

To create a counter rotation of the field requires us to choose $\beta = odd$ in conjunction with $\alpha = even$. Since $\alpha \geq 4$ there are no constraints on the values β may take.

In this case we find that we have an oppositely directed twist in the field which is localised to two squashed tori such that, once again, there is no twist in the fan plane. On either side of the fan plane the current density is equally directed but still of a similar general form as the previous z dependent symmetric case.

We also note that the flows above and below the fan are opposite to each other such that in the fan plane the plasma is static suggesting no flux is reconnected at the fan plane by this perturbation.

B. Torsional Fan

We now consider a current term localised in height z. It is convenient to choose $\alpha = 1$, $a = 0$ and $b = 1$ in equation (10) to yield field of the form

$$\mathbf{B} = B_0 \left(r, jr(zr^2)^\beta z^\gamma \mathrm{e}^{-\frac{z^2}{l^2} - \frac{c^2}{l^2}(zr^2)^2}, -2z \right) \tag{20}$$

where β and γ are positive integers. Using equation (7) the field line equations are

$$r = r_0 e^{B_0 s}, \quad z = z_0 e^{-2B_0 s}, \tag{21}$$

and

$$\phi = j B_0 (z_0 r_0^2)^\beta e^{-\frac{c^2}{l^2}(z_0 r_0^2)^2} G(\gamma) + C \tag{22}$$

where C is a constant of integration and $G(A)$ is defined as

$$G(A) = z_0^A \int e^{-2AB_0 s} e^{-\frac{z_0^2}{l^2} e^{-4B_0 s}} ds. \tag{23}$$

The recurrence relation for $G(A)$ is

$$G(A+2) = \frac{l^2}{2} \left(A G(A) + \frac{z^A}{2B_0} e^{-\frac{z^2}{l^2}} \right) \tag{24}$$

where we can generate solutions for all values of A from

$$G(1) = -\frac{\sqrt{\pi} l}{4 B_0} \mathbf{erf}\left(\frac{z}{l}\right) \tag{25}$$

$$G(2) = \frac{l^2}{4 B_0} e^{-\frac{z^2}{l^2}}. \tag{26}$$

Using equation (4) we find the current

$$\mathbf{J} = \frac{j B_0}{\mu_0} \left(-\left((\gamma + \beta) z^{-1} - \frac{2}{l^2} \left(z + c^2 (z r^2)^2 z^{-1} \right) \right), 0, 2(1+\beta) r^{-1} - \frac{4 c^2}{l^2} (z r^2)^2 r^{-1} \right) r z^\gamma (z r^2)^\beta e^{-\frac{z^2}{l^2} - \frac{c^2}{l^2}(z r^2)^2} \tag{27}$$

and equation (6) gives us the electric potential as

$$\Phi = \frac{j \eta_0 B_0}{\mu_0} \left[z r^2 \left(\left((\gamma + \beta) - \frac{2 c^2}{l^2} (z r^2)^2 \right) G(\gamma - 2) - \frac{2}{l^2} G(\gamma) \right) \right.$$
$$\left. + 2 \left(2(\beta + 1) - \frac{4 c^2}{l^2} (z r^2)^2 \right) G(\gamma + 1) \right] (z r^2)^\beta e^{-\frac{c^2}{l^2}(z r^2)} \tag{28}$$

It is clear that $\gamma \neq 0$ or 2 but there are no such constraints on β. In a similar manner to the previous section we now investigate further reconnection brought about by different choices of the various parameters.

1.   Opposite direction twist

It is clear from equation (20) that to perturb the field in this way we need $\gamma + \beta$ to be odd i.e. $\gamma = odd$ and $\beta = even$ or $\gamma = even$ and $\beta = odd$. A choice of the latter results in flows containing sinks and sources similar those in the torsional spine, $\alpha = odd$ case. We therefore only investigate in detail the $\gamma = odd$ and $\beta = even$ possibility.

The linear perturbation: $\beta = 0$ and $c = 0$.

In this case

$$\phi = j B_0 G(\gamma) + C. \tag{29}$$

The $\gamma = 1$ case is a special case with a non-zero current that linearly increases with r in the fan plane which makes it different from the generic case of $\gamma \geq 3$. Thus we shall study the more generic case whilst pointing out any differences from the special case of $\gamma = 1$. Let us consider $\gamma = 3$ for which the field is given by

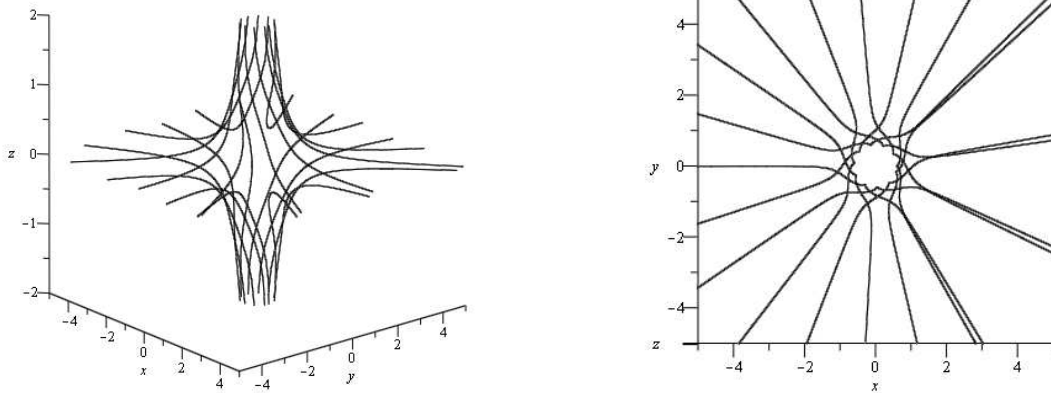$$\mathbf{B} = B_0 \left(r, j r z^3 e^{-\frac{z^2}{l^2}}, -2z \right). \tag{30}$$

FIG. 5: Side and top view of fieldlines plotted for $\gamma = 3$, $\beta = 0$, $j = 5$, $c = 0$ and $h = 1$. The field on the spine line is approaching the null and receding away from the null in the fan plane.
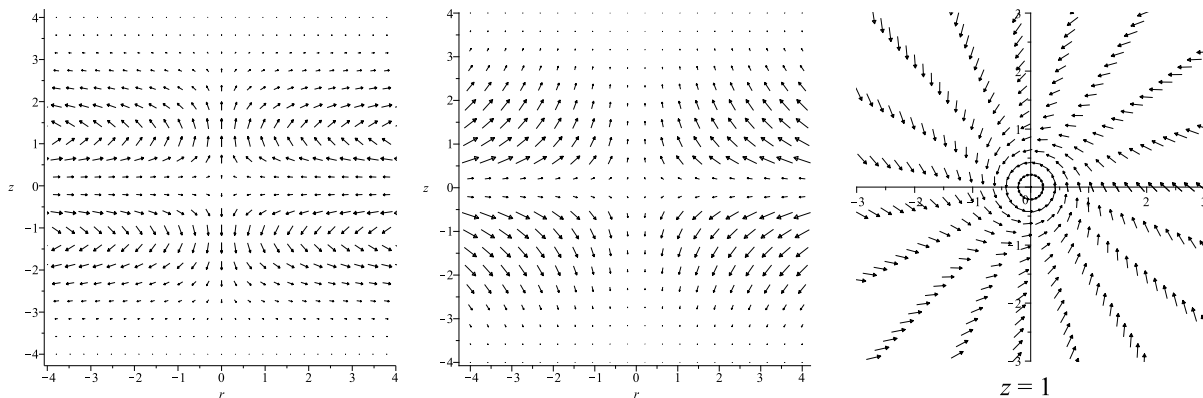

FIG. 6: Scaled plots of the radially symmetric current flow (left panel) and plasma flow (middle and right panels). Plotted for $\gamma = 3$ and $\beta = 0$ with $l = 1$, $c = 0$ and $j = 5$.

Figure 5 shows how the twist in the field above and below the fan is localised to two flattened toroidal disk-like regions above and below the fan plane. In Figure 6 we see that the resulting current is localised to this region of twist and exists in two disks of opposite current within each of the twisted regions. Current disks of this kind were observed by [18].

Figure 6 (middle and right panels) shows the plasma flow. This flow counter rotates below the fan with static plasma in the fan plane separating the two regions. As a result of this, we have counter spiraling flows that move in along the fan and then spiral out close to the spine. Comparing to Figure 2 we note that in the positive rz-plane the flows are in the opposite direction to torsional spine. As expected the flow is strongest in the two disc-like twisted regions.

Note that the effect of increasing γ to higher odd values is to increase (decrease) the twist where $z > l$ ($z < l$) in an analogous way to the torsional spine case. Similarly increasing l also serves to reduce the damping of the exponential term with height and therefore to stretch the solution in z.

The nonlinear perturbation: $\beta \neq 0$ and $c \neq 0$.

Here we consider $\beta \neq 0$ and *even*. Since we are prohibited to choose $\gamma = 0$ (see equation (28)) we consider
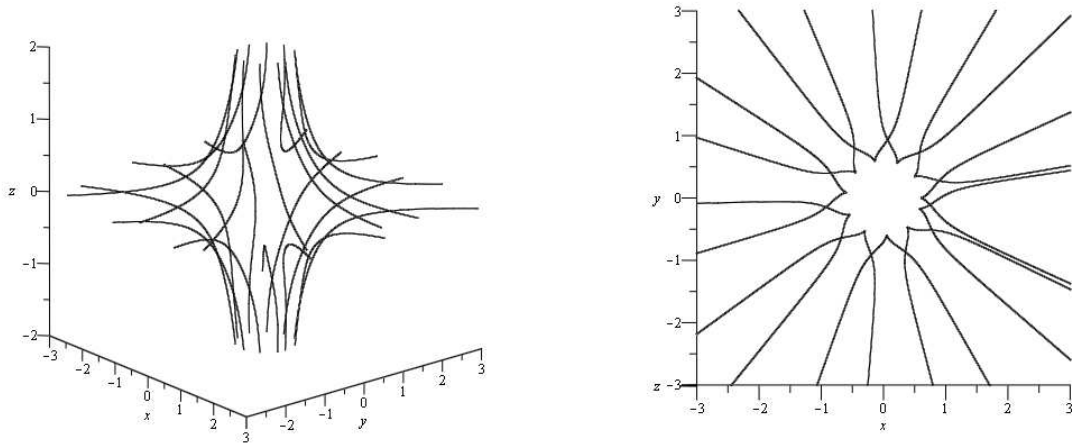
FIG. 7: Side and top view of fieldlines plotted for $\gamma = 3$, $\beta = 2$, $j = 5$, $l = 1$ and $c = 0.2$. The field on the spine line is approaching the null and receding away from the null in the fan plane.

the previous case of $\gamma = 3$ combined with $\beta = 2$ and a non-zero c value to maintain locality giving a field of the form

$$\mathbf{B} = B_0 \left(r, jr^4 z^5 e^{-\frac{z^2}{l^2} - \frac{c^2}{l^2}(zr^2)^2}, -2z\right). \tag{31}$$

The resulting field lines are shown in Figure 7. The twist in the fieldlines is differentially varying with radius and localised to within two squashed tori on either side of the fan. Like the torsional spine case this is due to the extra damping i.e. $c \neq 0$.

Figure 8, left panel, shows the resulting current that is localised to this region and rotates around within it. The middle and right panels of the figure show the plasma flow. The flows are much more complex than in the linear case. The original flow is sandwiched by counter rotating flows from below and above. The flow in the vicinity of the fan plane results from the non-linearity in r of the power law in the perturbation i.e. through $\beta \neq 0$. This new flow spans both the spine and the fan becoming infinitely thin far away from the null, i.e. only the fan and the spine themselves. The second flow is a result of the non-linearity in r of the exponential from $c \neq 0$. These flows are effectively the non-linear radial nature of torsional spine reconnection asserting itself in the torsional fan regime.

Lastly the $\gamma = 1$ case behaves differently from the more generic cases of $\gamma \geq 3$. The smaller value of γ means that there is a linear flow ($\beta = c = 0$) down around the spine and out along the fan in the same manner as in the torsional spine reconnection. Therefore when the perturbation is made nonlinear in r the new flow is lost within the original one. We do however still see a counter rotating flow because of $c \neq 0$ but it is counter rotating in relation to the first flow and therefore, is in the more generic direction for fan reconnection, along the fan and up the spine. Figure (9) illustrates this for the example of $\gamma = 1$, $\beta = 2$ and $c = 0.2$.

So the overall picture of the plasma flow for the most generic, radially differentially varying counter twist, is a counter rotating spiraling flow, the majority of which travels along the fan and up around the spine with a portion of it counter rotating in relation to this first flow down the spine and out along the fan in two distinct regions. Static plasma in the fan separates the positive and negative z regions.

2. Same direction twist

As mentioned earlier the choice of $\gamma = even$ is not a realistic solution to the problem so we consider γ and β both *odd* for this case. As an example, let

$$\mathbf{B} = B_0 \left(r, jr^3 z^4 e^{-\frac{z^2}{l^2} - \frac{c^2}{l^2}(zr^2)^2}, -2z\right). \tag{32}$$

where $\gamma = 3$ and $\beta = 1$ yields same direction field lines in the rz-plane. Such field lines result in a current density which is oppositely directed on either side of the fan plane whilst still being localised in a similar way to the previous
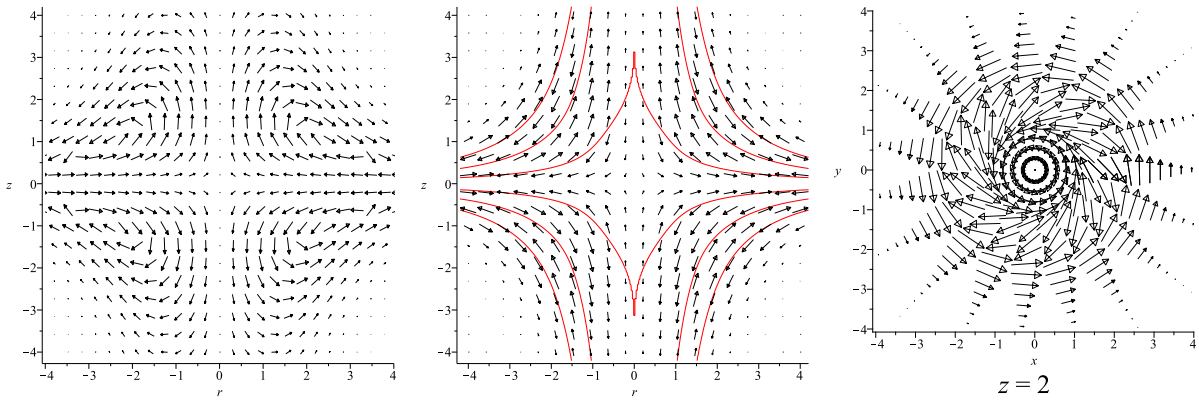
FIG. 8: The left panel shows a slice of the scaled radially symmetric current flow, the middle and right panels showing the side and top views respectively of the scaled plasma flow when $\gamma = 3$, $\beta = 2$ and $c = 0.2$ with $l = 1$ and $j = 5$ where $d = 13$.
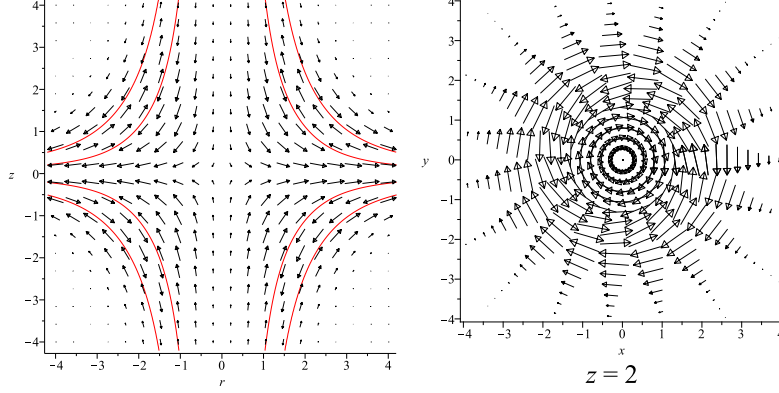

FIG. 9: Top and side view of the scaled radially symmetric plasma flow for $\gamma = 1$, $\beta = 2$ and $a = 0.2$ with $l = 1$ and $j = 5$ where $d = 13$.

current in Figure 8. The plasma flows are again found to be counter rotating flows of the generic type described in the previous section except now the flow is equally directed either side of the fan allowing for a rotating flow in the fan itself. Again for the $\gamma = 1$ case the new flow is lost within that of the original due to it's different directional nature.

IV.   DISCUSSION

We have seen that for a twisting perturbation of the field around a 3D null current localises to a torus within the perturbed region of field driving a slippage of the plasma though this region. Flux transport is therefore heavily dependent on the localisation of the perturbation. The two main cases being that of localisation around the spine or the fan. We have seen that the inclusion of terms with non-linearity in r lead to torsional spine type flows and terms with non-linearity in z lead to torsional fan type flows. Thus, we expect a smooth transition from one to the other. This requires an intermediate step: when $a = b = \gamma = \alpha = 0$ with $c = \beta \neq 0$, resulting in a field of the form

$$\mathbf{B} = B_0 \left(r, j(zr^2)^\beta e^{-\frac{c^2}{l^2}(zr^2)^2}, -2z \right) . \tag{33}$$

A field of this form is perturbed in a way which has no bias to either spine or fan but varies differentially in zr^2. In this case both electric potentials reduce to

$$\Phi = \frac{j\eta_0 B_0}{3\mu_0} \left(\left(\beta - \frac{2c^2}{l^2}(zr^2)^2 \right) \frac{r}{z} + 2 \left(2\beta + 1 - \frac{4c^2}{l^2}(zr^2)^2 \right) \frac{z}{r} \right) (zr^2)^\beta e^{-\frac{c^2}{l^2}(zr^2)^2} \tag{34}$$
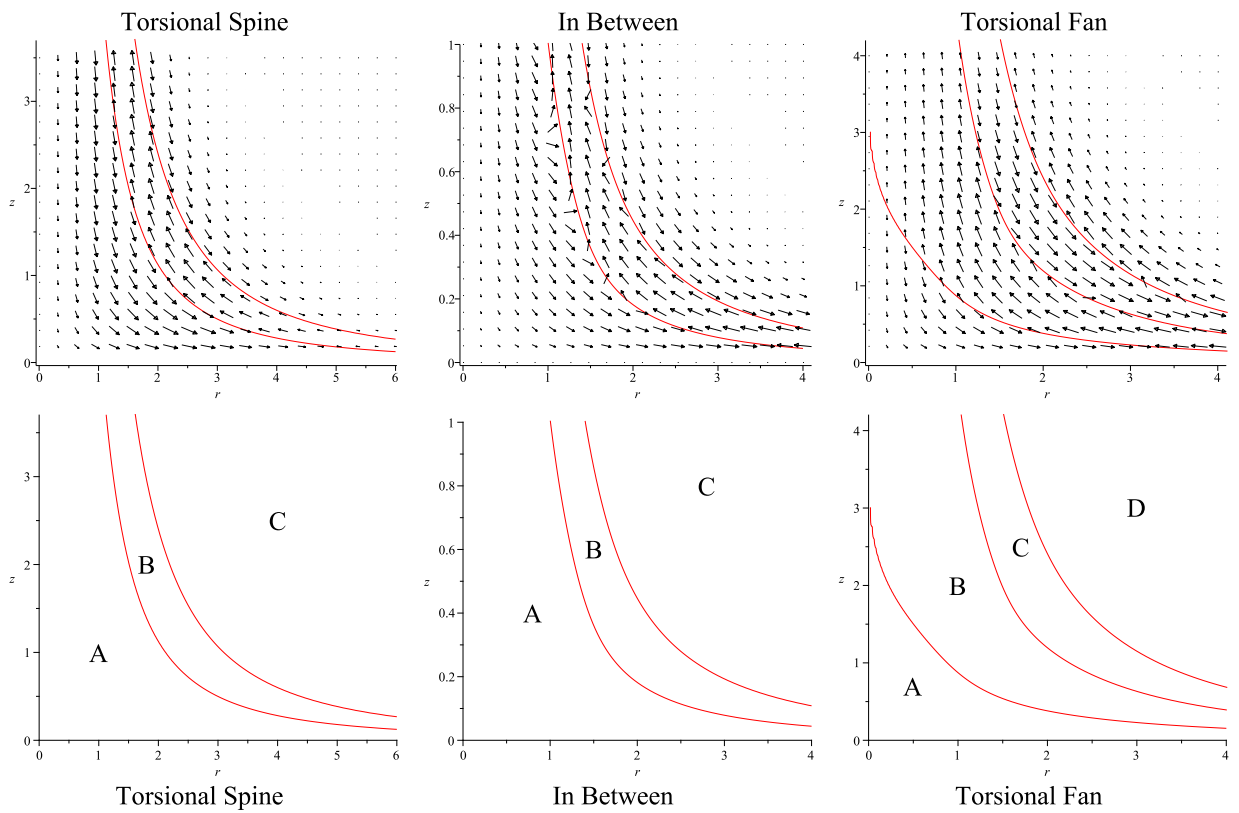
FIG. 10: Flux transport regions in the positive rz-plane for the torsional spine ($\beta \neq 0$ and $c \neq 0$) and fan ($\beta \neq 0$, $\gamma \geq 3$ and $c \neq 0$) cases and the connecting regime between them. The top row shows the plasma direction whilst the bottom row seperates regions in each regime. The solid red lines denote where $v_{\perp z} = 0$

Figure (10) shows how the two cases are linked by this term by focusing on the plasma flow in the positive rz-region since the direction of twist in this region remains the same for all values of α, γ and β. The region **A** corresponds to pure z-independent torsional spine flow, **B** corresponds to pure linear torsional fan flow and **C** and **D** are associated with the damping from $c \neq 0$. We see how most of these flows appear in each case.

V.   CONCLUSION

We investigated torsional magnetic reconnection at a 3D null point by allowing perturbations in the ϕ component of the magnetic field. We introduced models for the *Torsional Spine* and *Torsional Fan* reconnection regimes through solutions of the steady state kinematic resistive MHD equations. In both regimes we found spiral slippage of the field lines around the spine where we noted that this slippage is not involved in the flux transport across the spine or the fan. We also found from the nature of the twist in the field that current was focused around the spine for torsional spine and at the fan for torsional fan.

We then investigated twists with non-linearity in both r and z. The flows are found to be complex with competing effects between the two non-linearities. We then linked the two main cases with an intermediate step indicating that each of the 'pure' linear regimes of Torsional Spine and Fan are extreme cases of a general twist in the field.

[1] G. Barnes, Astrophys. J. Lett., 670, L53-L56 (2007)

[2] I. J. D. Craig, R. B. Fabling, J. Heerikhuisen, & P. G. Watson, ApJ, 523, 838-848 (1999)

[3] K. Galsgaard, & A. Nordlund, J. Geophys. Res., 102, 231-248 (1997)

[4] K. Galsgaard, E. R. Priest & V. S. Titov, J. Geophys. Res., 108 (A1), 1042 (2002)

[5] Y. T. Lau, & J. M. Finn, Astrophys. J., 350, 672-691 (1990)

[6] D. W. Longcope, Solar Phys., 169, 99-121 (1996)

[7] D. W. Longcope, & S. C. Cowley, Phys. Plasmas, 3, 2885-2897 (1996)

[8] D. W. Longcope, Phys. Plasmas, 8 5277-5290 (2001)

[9] D. W. Longcope, & I. Klapper, Astrophys. J., 579, 468-481 (2002)

[10] D. W. Longcope, D. S. Brown, & E. R. Priest, Phys. Plasmas, 10, 3321-3334 (2003)

[11] D. W. Longcope, & C. E. Parnell, Solar. Phys., 254, 51-75 (2009)

[12] M. L. Luoni, H. H. Mandrini, G. D. & P. Démoulin, Adv. Space Res., 39, 1382-1388 (2007)

[13] S. Masson, S., E. Pariat, G. Aulanier, & C. J. Schrijver, Astrophys. J., 700, 599-578 (2009)

[14] E. Pariat, S. K. Antiochos & C. R. De Vore, Astrophys. J., 691, 61 (2009)

[15] D. I. Pontin, G. Hornig, & E. R. Priest, Geophys. Astrophys. Fluid Dynamics, 98, 407-428 (2004)

[16] D. I. Pontin, G. Hornig, & E. R. Priest, Geophys. Astrophys. Fluid Dynamics, 99, 77-93 (2005)

[17] D. I. Pontin, & I. J. D. Craig, Phys. Plasmas, 12 (072112), (2005)

[18] D. I. Pontin, & K. Galsgaard, J. Geophys. Res., 112, (3103) (2007)

[19] D. I. Pontin, & E. R. Priest, Phys. Plasmas 16, (122101) (2009)

[20] E. R. Priest, & V. S. Titov, Phil. Trans. R. Soc. Lon. A, 354, 2951-2992 (1996)

[21] E. R. Priest, G. Hornig & D. I. Pontin, J. Geophys. Res., 108(A7), 1285 (2003)

[22] S. Regnier, C. E. Parnell, & A. L. Haynes, Astron. Astrophys., 484, L47-L50 (2008)

[23] T. Török, G. Aulanier, B. Schmieder, K. K. Reeves, & L. Golub, Astrophys. J., 704, 485-495 (2009)

[24] I. Ugarte-Urra, H. P. Warren, & A. R. Winebarger, Astrophys. J., 662, 1293-1301 (2007)

[25] C.J. Xioa, X. G. Wang, Z. Y. Pu, H. Zhao, J. X. Wang, Z. W. Ma, S. Y. Fu, M. G. Kivelson, Z. X. Liu, Zong, Q. G., Glassmeier, G. H., Balogh, A., Korth, A., Reme, H. & Escoubet, C. P. 2006, , Nature., 2, 478-483 (2006)